Langmuir

Article

pubs.acs.org/Langmuir

Adsorption of F127 onto Single-Walled Carbon Nanotubes Characterized Using Small-Angle Neutron Scattering

E. S. Kastrisianaki-Guyton,*[,†] L. Chen,[‡] S. E. Rogers,[§] T. Cosgrove,[†] and J. S. van Duijneveldt*[,†]

[†]School of Chemistry, University of Bristol, Cantock's Close, Bristol BS8 1TS, United Kingdom

[‡]Merck Chemicals Ltd., Chilworth Technical Centre, University Parkway, Southampton SO16 7QD, United Kingdom

[§]ISIS Neutron Source, STFC Rutherford Appleton Laboratory , Didcot, Oxfordshire, OX11 0QX, United Kingdom

Supporting Information

ABSTRACT: Aqueous single-walled carbon nanotube dispersions are often made using polymers from the pluronic family of amphiphilic block copolymers; however, relatively few studies have been conducted using small-angle neutron scattering techniques to discover the mechanism by which they act. SANS results reported here show that a relatively simple core−shell cylinder model can be used to fit data successfully at different contrasts. The results across all contrasts showed that the best fit gave an inner nanotube radius of 10 Å, corresponding to small nanotube bundles with a small amount of water present (20%), and a polydisperse adsorbed layer thickness of 61 Å, with a water content of 94% in the adsorbed layer. The data fitting is thus consistent with a small SWCNT bundle surrounded by an extended and water-swollen F127 adsorbed layer. Comparing the scattering from F127/SWCNT at different contrasts, it has been found that the polymer-decorated SWCNTs are contrast matched at a D_2O/H_2O volume ratio of 0.36:0.64, corresponding to a scattering-length density of 1.92×10^{-6} Å^{-2}.

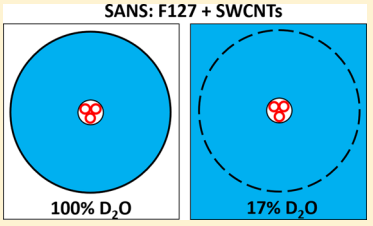

INTRODUCTION

Carbon nanotubes have been of great interest since their discovery by Iijima in 1991 as a result of their unique properties such as their high aspect ratio, mechanical strength, and electrical conductivity.[1] Single-walled carbon nanotubes (SWCNTs) can be thought of conceptually as a rolled-up sheet of atomically thin carbon, with both the angle used when rolling up this cylinder and the diameter of the resulting nanotube being key parameters in determining its electronic properties. Syntheses of SWCNTs result in a third of the nanotubes being metallic, with two-thirds being semiconducting.[2] There has been a surge in research interest in recent years looking into possible separation methods for these two species of nanotubes in order to make SWCNTs of a single electronic type for future electronic applications.

A major challenge in utilizing the properties of SWCNTs is the difficulty encountered on attempting to form a nanotube dispersion in either aqueous or organic media as a result of the propensity of SWCNTs to bundle together. Methods which have been investigated to overcome this problem include both covalent and noncovalent approaches, with noncovalent methods generally being favored as they do not affect the intrinsic properties of the SWCNTs.

A variety of both small molecule and polymeric surfactants have been reported as forming SWCNT dispersions successfully. Interactions between surfactant molecules and the SWCNT surface occur with the adsorption of the hydrophobic tail of the surfactant onto the SWCNT wall. Although such dispersants are commonly used with SWCNTs, relatively few studies have utilized small-angle neutron scattering (SANS) as a technique to investigate the adsorption of surfactants onto SWCNTs. Yurekli et al. studied the adsorption of sodium dodecyl sulfate (SDS) on CNTs at low surfactant concentration using SANS and reported that the adsorption of SDS molecules on the SWCNT surface was unstructured, with no preferential adsorption of either the headgroup or the tail of the molecule onto the SWCNT wall.[3] Theoretical calculations have shown that in dilute solution the adsorption of surfactant on the tube is random in nature while at high surfactant concentration hemispherical micelles are preferentially formed.[4] The stabilization of carbon black and SWCNTs has been reported to be more effective with the use of surfactants possessing aromatic groups, due to $\pi-\pi$ stacking interactions between the surfactant and the graphitic carbon surface.[5,6]

Work published by Granite et al. looked into using SANS to probe the interactions between SWCNTs and pluronic block copolymers (F127 and F108) below the polymers' critical micellization temperature (CMT).[7] They observed minimum scattering at 70% D_2O rather than at 17% D_2O, which is where the pluronic polymers would be expected to be "matched out" based on their chemical structure. Both a cylindrical core-adsorbed chains model and a cylindrical core−shell−chains model were reported as fitting the data well; however, corrections had to be made as to why the data at 70% D_2O scattered less than the data at 40% D_2O, a value which is closer to the match point of F127.

We have studied the adsorption of F127 onto SWCNTs using SANS and have found our data to show a different

Received: January 29, 2015
Revised: February 19, 2015
Published: February 21, 2015

DOI: 10.1021/acs.langmuir.5b00375
Langmuir 2015, 31, 3262−3268

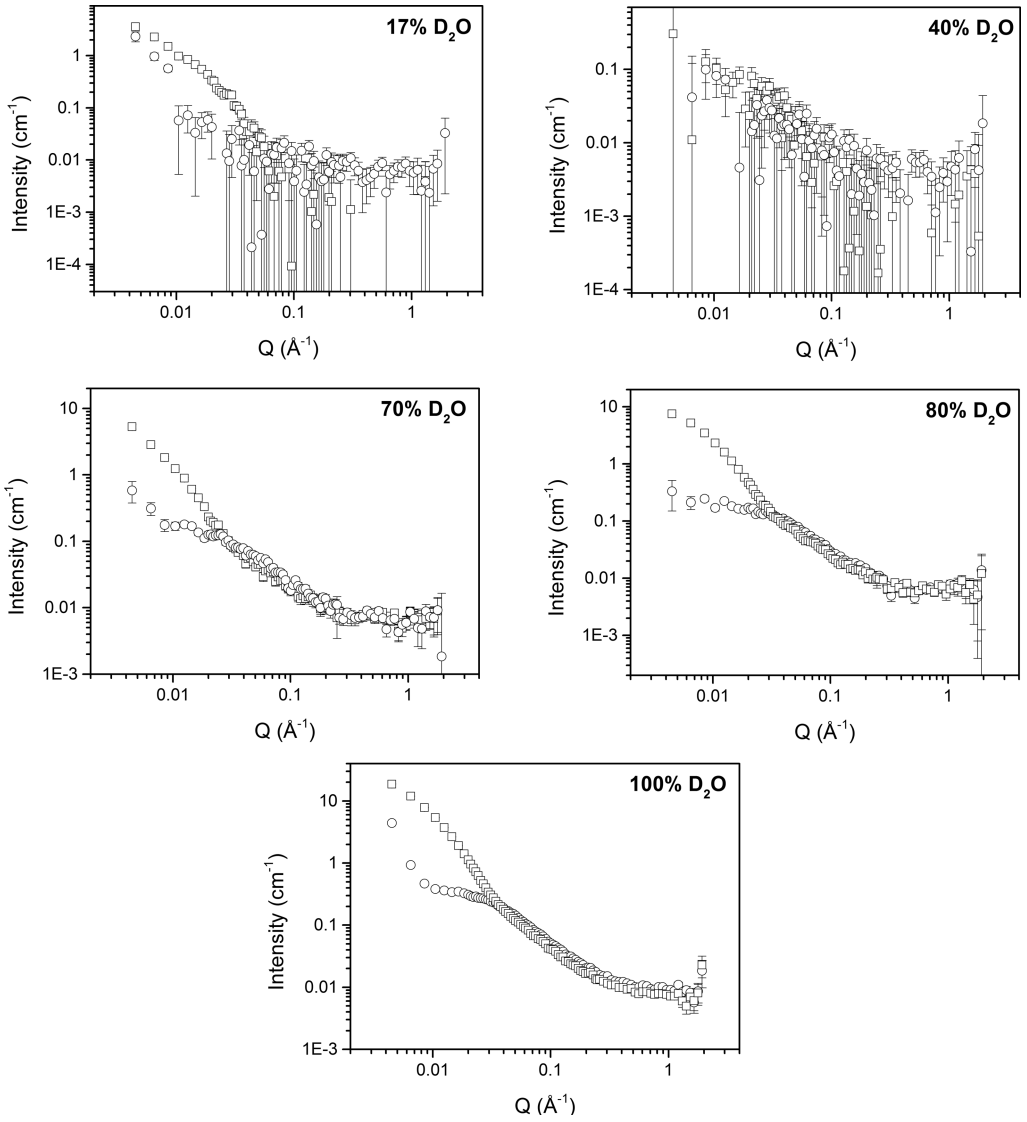

Figure 1. SANS scattering curves from dispersions of 1% w/w F127 (○) and 1% w/w F127 with 0.3% w/w SWCNTs (□).

scattering vector (Q) dependency than previous data. Our data show minimal scattering at a D_2O/H_2O composition consistent with a model in which the SWCNT has a high scattering-length density and is surrounded by a diffuse F127 adsorbed layer. We have found it possible to obtain good fits to our F127/SWCNT data using a relatively simple core−shell cylinder model.

EXPERIMENTAL SECTION

Materials. Single-walled carbon nanotubes (SWCNTs) synthesized by a high-pressure carbon monoxide (HiPCO) method were purchased from NanoIntegris ("purified" grade). F127 was obtained from BASF (Ludwigshafen, Germany). D_2O was purchased from Sigma-Aldrich (99.9 atom % D).

Preparation of Dispersions. Sample preparation involved dissolving the polymer in water (either hydrogenated or deuterated) overnight while on a roller mixer. All samples were made by the addition of the required mass of SWCNTs to 2 mL of a polymer solution of the correct concentration to obtain a dispersion which was 0.3 wt % SWCNTs and 1 wt % F127. This was followed by sonication (QSonica Q125) in pulsed mode at 57% max power for 1 h. The samples were then centrifuged for 40 min at 20 800 g, and the top ∼1.5 mL of the resulting supernatant was removed for use in scattering experiments. It is important to note that the SWCNT concentration of 0.3 wt % quoted is not the final concentration but rather is the concentration calculated before purification by ultracentrifugation. It is estimated from absorption measurements that approximately one-third of the SWCNTs remain dispersed after purification, a relatively high concentration thought to be a consequence of the high purity of SWCNTs used.

Absorption Spectroscopy. Absorption spectroscopy was performed on an HP/Agilent 8453 spectrophotometer over the range of 400−1100 nm. Samples were diluted by a factor of 30 with deionized water and run in square quartz cells with a 10 mm path length. Background water absorption was subtracted from all data.

Small-Angle Neutron Scattering. Small-angle neutron scattering experiments were performed on the SANS2D small-angle diffractometer at the ISIS pulsed neutron source (STFC Rutherford Appleton Laboratory, Didcot, U.K.). A collimation length of 4 m and an incident wavelength of 1.75−16.5 Å were used. Data were measured simultaneously on two 1 m^2 detectors to give a Q range of 0.0045−1.92 $Å^{-1}$. The small-angle detector was positioned 4 m from the sample and offset vertically 60 mm and sideways 100 mm. The wide-angle detector was positioned 2.4 m from the sample, offset sideways by 980 mm, and rotated to face the sample. The beam diameter was 8 mm. Each raw scattering data set was corrected for the detector efficiencies, sample transmission, and background scattering and converted to scattering cross-section data ($\delta\Sigma/\delta\Omega$ vs Q) using instrument-specific software.[8] These data were placed on an absolute scale (cm^{-1}) using the scattering from a standard sample (a solid blend

DOI: 10.1021/acs.langmuir.5b00375
Langmuir 2015, 31, 3262−3268

of hydrogenous and perdeuterated polystyrene), in accordance with established procedures.[9]

Samples were studied in 2 or 1 mm square quartz cells depending on the D_2O/H_2O content. All samples were studied below the critical micellization temperature (CMT) to minimize scattering from the bare polymer. For an F127 concentration of 1% w/v, as used here, the CMT is 24 °C.[10] Therefore, samples were studied at 15 °C. All data sets had background solvent scattering subtracted.

To ensure the F127/SWCNT samples contained the same amount of carbon (to simplify the SANS data analysis), the samples were made from F127/SWCNT/D_2O and F127/SWCNT/H_2O stock solutions which were mixed together in the correct proportions. The stock solutions were made as described previously to give a total volume for the stock solution of over 1 mL. The concentrations of the two stock solutions were then compared using absorption spectroscopy, and the more concentrated D_2O solution was diluted to the same concentration as the H_2O stock solution dilution with a 1% F127 solution until the absorption spectra of the two stock solutions matched.

RESULTS AND DISCUSSION: SMALL-ANGLE NEUTRON SCATTERING

The scattering patterns from dispersions of F127 polymer along with the F127/SWCNT data at the contrasts studied are given in Figure 1. As all dispersions were studied below the CMT of the polymer, F127 did not form micelles and was instead present as free polymer chains, and thus the scattering contribution from F127 itself was relatively small. At low Q values, the data for the F127/SWCNTs has a higher scattering intensity than F127; however, at high Q the curves have very similar shapes, suggesting that the scattering at high Q is dominated by the free F127 molecules. The curves for F127/SWCNTs tend to be at a lower intensity than for F127 alone at higher Q, suggesting that some of the F127 has adsorbed onto the SWCNT surface, which is thus affecting the scattering intensity in this Q range. The scattering data shows the highest-intensity scattering at 100% D_2O, as expected, with 80 and 70% D_2O data both showing scattering of a lower intensity than the full contrast data. The minimal scattering for our samples is seen at 40% D_2O, with some scattering seen at the lowest Q values for the 17% D_2O data (the match point of the F127), corresponding to the scattering of the nanotubes themselves with the F127 adsorbed layer matched to the solvent.

Data for F127 were fit to a Debye–Guinier model for free polymers, which was then subtracted from the F127/SWCNT data. Details about the fitting procedure are given in the Supporting Information for this article. Data for SWCNT/F127 showed lower-intensity scattering at high Q, so only 75% of the F127 Debye-Guinier fit was subtracted from the F127/SWCNT data to account for F127 adsorption onto SWCNTs, and the resulting scattering curves are shown in Figure 2.

The scattering patterns of the F127/SWCNT samples at different contrasts are shown in Figure 2. The scattering results presented here show that for the F127/SWCNT samples the minimal scattering is seen at 40% SWCNT, as would be expected for a core–shell cylinder of this type. F127 alone is contrast matched at 17% D_2O, the data for which is shown in Figure 1, and at this contrast the F127/SWCNT data shows a Q^{-1} power law at low Q, indicating that rod-shaped objects are present.

A contrast match plot for the F127/SWCNT data was made by taking the intensity of the SWCNT/F127 scattering at a Q value of 0.0085 $Å^{-1}$ and subtracting the incoherent background and the F127 scattering at this contrast. The resulting contrast

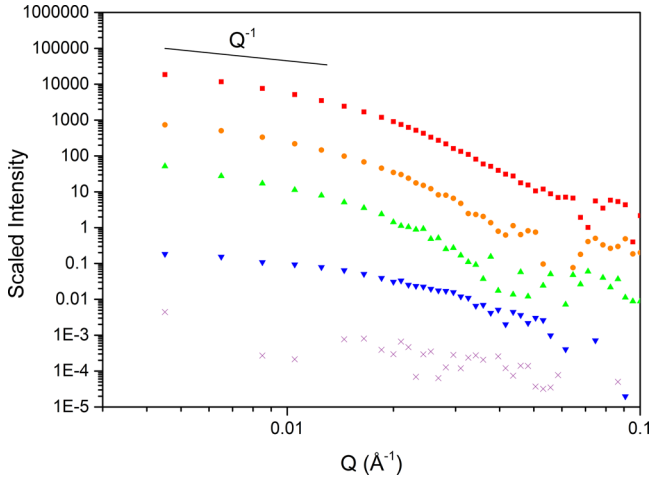

Figure 2. SANS data from F127/SWCNT systems at various contrasts, with background D_2O and 0.75× the F127 scattering subtracted, after shifting data sets for clarity. Each data set was shifted by a factor of 10 away from the data set next to it. D_2O content: 100% (red ■), 80% (orange ●), 70% (green ▲), 40% (purple ×), and 17% (blue ▼).

variation graph is shown in Figure 3. The data point at 17% D_2O was beyond the contrast point and thus had an intensity

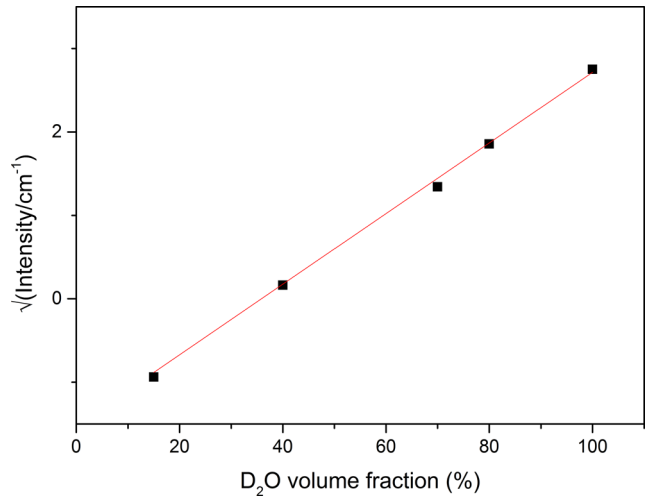

Figure 3. Contrast match plot for F127/SWCNT samples run at different contrasts. The intensity at $Q = 0.0085$ $Å^{-1}$ was used for every contrast studied, and the background scattering and F127 scattering at this Q value were subtracted.

above that of the 40% D_2O data. Ideally, two separate lines would be drawn (above and below the match point) in order to find the x intercept and thus the contrast match point; however, in this case only one of the contrasts studied was at a D_2O composition below the match point. Thus, the intensity value at 17% D_2O was multiplied by a factor of −1 to enable one straight line to be drawn. The data shows a good fit to a straight line, and it can be concluded that a volume fraction of 36% D_2O would be required in order to obtain the minimal scattering from this system. This is in contrast to results reported by Granite et al., who observed a minimal scattering at 70% D_2O. Subtracted data shown in Figure 6 shows that the scattering for the SWCNTs shows a Q^{-1} power law at low values of Q, whereas Granite et al. reported a higher power law

DOI: 10.1021/acs.langmuir.5b00375
Langmuir 2015, 31, 3262–3268

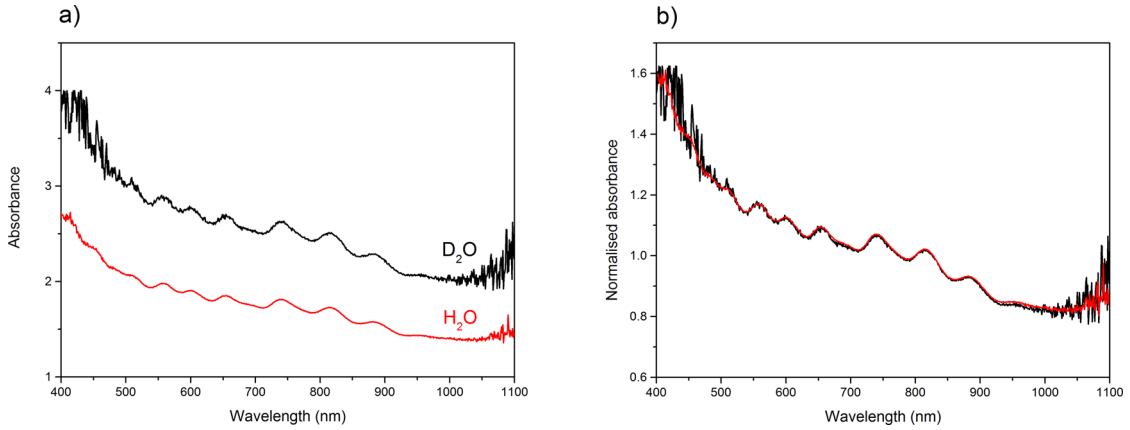

Figure 4. Absorption spectra of F127/SWCNT/D_2O (black line) and F127/SWCNT/H_2O (red line) dispersions, with both the original spectra (a) and the spectrum with the absorbances normalized at 800 nm (b).

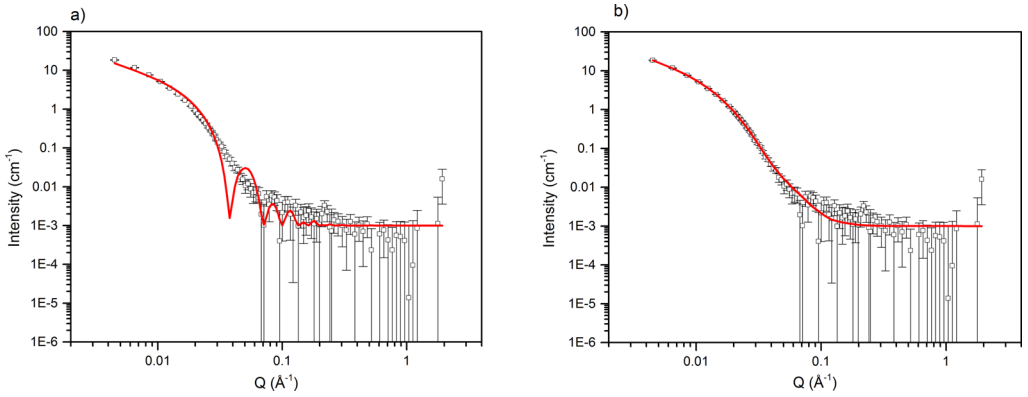

Figure 5. Fitting procedure. Thickness: (a) no polydispersity; (b) polydispersity added to the thickness of the adsorbed layer.

relation attributed to branching of SWCNTs and a wide range of SWCNT sizes. It is thus possible that dispersions made here have a lower degree of SWCNT branching and are thus more amenable to being fit to a core–shell cylinder model.[7,11,12]

Judging from previous experiments looking at the dispersions using TEM (shown in the Supporting Information for this article), it is unlikely that the SWCNTs will be present as individual tubes, although some of them may be. Rather, the majority of the nanotubes will be present in small bundles. TEM images also show that residual catalyst particles are present in the dispersions; however, this is not thought to affect the SANS results, as explained further in the Supporting Information for this article.

It has been reported that the degree of bundling in a sample can be detected by UV–vis–NIR spectrophotometry.[13] SWCNT bundling causes broadening and red shifting of the peaks in the UV–vis–NIR spectra.[14] The absorption spectra obtained from our samples, shown in Figure 4, have peaks which are not as sharply defined as the single SWCNT peaks in Backes et al.'s work, implying that some degree of bundling is present. However, absorption spectra of the samples are similar to those seen by Yurekli et al., who took these as evidence that the SWCNTs were present as individual tubes rather than bundles.[3] The absorption spectra of the F127/SWCNT systems in D_2O and H_2O were scaled down by dividing all absorbances by the absorbance obtained at 800 nm. Thus, the peaks of the absorption spectra can be directly compared, and it is clear that the spectra show very similar absorbance peaks, suggesting that the level of debundling is similar in both samples.

The model used to fit the data presented here is a core–shell cylinder model, simpler than models previously used to fit such data, and the scattering-length densities (of the core and shell) are averaged with the relative amount of water thought to be present, as explained in the Supporting Information.

We have used a core–shell cylinder model to fit the scattering data of the decorated SWCNT cylinders at all contrasts studied, using the SasView fitting program developed at NIST.[15] This model consists of a core (with an SLD calculated as a mixure of the SLD of graphene, calculated to be 7.4×10^{-6} Å^{-2}), the scattering-length density of the appropriate solvent mixture, and a homogeneous shell consisting of a diffuse F127 layer. To simulate the inhomogeneity of the F127 adsorbed layer in this simple model, a log-normal polydispersity for thickness has been introduced into the scattering of the shell. The polydispersity function used also serves to account for the instrument resolution, as the Q dependency of the data is weak and smearing due to polydispersity is much greater than the effect of the instrument resolution.

Adsorbed layers of F127 have been widely studied, and the values obtained for the size and composition of these adsorbed layers give an idea of what the contribution to scattering from the adsorbed layer in the system studied here is likely to be. Granite et al. estimated that the adsorbed layer of F127 on their SWCNT samples had a thickness of 120 Å and a volume fraction of 0.049, which corresponds to an adsorbed amount of 1.80 mg m^{-2}.[7] Malmsten et al. studied F127 adsorption at silica surfaces and found the hydrodynamic thickness of the layer to be 20–60 Å.[16] Assuming a thickness of 60 Å, the volume

DOI: 10.1021/acs.langmuir.5b00375
Langmuir 2015, 31, 3262–3268

fraction of F127 in the layer would need to be 0.07 in order to match the adsorbed amount of 0.4 mg m^{-2}. Lin and Alexandridis measured an F127 layer thickness of 71 Å on carbon black and the adsorbed amount to be 0.543 mg m^{-2}, while Nelson and Cosgrove found the adsorbed layer of F127 on laponite to have a thickness of only 35 Å with an adsorbed amount of 0.87 mg m^{-2}. It is therefore expected that the adsorbed F127 layer will have a relatively low volume fraction; however, the thickness could be anywhere in a wide range of reported values.[17,18] The adsorbed layer thickness must be less than the extended chain length of one of the PEO blocks (350 Å based on a monomer chain length of 3.5 Å[19]).

The fitting procedure used here consists of several stages. (1) The thickness of the adsorbed layer can be approximated using the scattering data obtained at 100% D_2O. We have assumed that the core has a high SLD (as we think it mainly consists of carbon, with some solvent present from the opening of the tubes during ultrasonication) and a relatively small radius. The shell is composed of a diffuse layer which has a high solvent composition. Therefore, at the highest D_2O content, the scattering-length density of the shell will nearly match the scattering-length density of the core, and fitting the shape of this data will depend mainly on the thickness of the adsorbed layer. Rather than using a model in which the adsorbed layer is "fuzzy", it was decided to use a simple model in order to keep the number of parameters at a minimum. Adding polydispersity to the thickness of the adsorbed layer has a similar effect to using a fuzzy-layer model and decreases the polymer segment density away from the core. This can be seen in Figure 5. Thus, a value of 61 Å was obtained for the F127 adsorbed layer, with a log-normal polydispersity of 0.4, the distribution of which is given in the Supporting Information. By integrating over the log-normal distribution, a mean thickness (taking into account the polydispersity) of 65 Å was obtained. (2) Once the thickness had been established, it could then be used to calculate the volume fraction of F127 in the adsorbed layer. The scattering intensity of SWCNT/F127 data at high Q was lower than that of F127 alone at every H_2O/D_2O composition, which was interpreted as being caused by a fraction of the F127 having been removed from the solution by adsorption onto SWCNTs. (3) Finally, Figure 3 shows that the contrast match point for the F127/SWCNT scattering occurs at 36% D_2O. The thickness and the volume fraction of the adsorbed layer are known; therefore, the scattering-length density of the SWCNT can be calculated so that the scattering from the core and the shell cancel each other out at this D_2O composition. Preliminary data fitting shows that the best fits are obtained with a relatively small core radius and a low volume fraction of water in the SWCNT core. We can use the relationship between the scattering of the core and shell to fit the data at different core radii and core SLDs (assuming different amounts of solvent are present in the core each time) in order to find the best fit across all contrasts studied. The contrast match point, shown in Figure 3 to be 36% D_2O, must satisfy the condition given in eq 1.

$$\rho_{core} a_{core} + \rho_{shell} a_{shell} = 0 \quad (1)$$

We have calculated the contribution to the overall scattering from the inner SWCNT core and the outer adsorbed layer based on the fitting parameters given in Table. 1. With an inner radius of 10 Å, an F127 shell thickness of 61 Å, a volume fraction of water in the shell of 0.94, and a volume fraction of water in the core of 0.2, the calculated match point would be 37% D_2O, a value which is very close to the value estimated from Figure 3.

Table 1. Table of Parameters Used to Fit SWCNT/F127 Data to the Core−Shell Cylinder Model across All Contrasts[a]

parameter	
water in core/vol %	20
water in shell/vol %	94
radius/Å	10
shell thickness/Å	61
polydispersity of thickness	0.43
volume fraction	0.049

[a]The values for $\rho_{solvent}$ are as follows: 17% D_2O, 0.5×10^{-6} $Å^{-2}$; 40% D_2O, 2.2×10^{-6} $Å^{-2}$; 70% D_2O, 4.27×10^{-6} $Å^{-2}$; 80% D_2O, 4.96×10^{-6} $Å^{-2}$; and 100% D_2O, 6.36×10^{-6} $Å^{-2}$.

Fitting the data to a core−shell cylinder model gives reasonable fits across all contrasts studied, as shown in Figure 6. The fits show the core to be a small SWCNT bundle surrounded by a diffuse, polydisperse layer of F127 with a thickness of 61 Å. The parameters used in fitting the data to a core−shell cylinder model are given in Table 1. The data at 17% D_2O could be fit by including a small amount of scattering in the shell (i.e., the shell was slightly off contrast) to account for imperfect contrast matching of the F127. Polydispersity was added to the thickness of the adsorbed layer in order to approximate the effect of the PEO and PPO blocks of the polymer. The data for the system at 40% D_2O has a very low scattering intensity and large error bars associated with it, and thus fitting this data is difficult. However, this is a key piece of evidence to support the core−shell cylinder model as it shows that the system is close to the match point at this D_2O content.

On the basis of the fits obtained here, the amount of F127 adsorbed was calculated and compared with the amount of F127 which had been assumed to be adsorbed to the SWCNT surface based on the subtracted surfactant data. The volume fraction of decorated cylinders, thickness of the adsorbed layer, and radius of the SWCNT bundle obtained from the fits were used to calculate the total length of the cylinders in the sample. The total amount of F127 used can then be calculated using the volume fraction of F127 in the adsorbed layer. Using this method, the total amount of adsorbed F127 is calculated to be 0.0022 g of adsorbed F127 per cm^3 sample, compared to 0.0025 g from the fraction of the F127 data which was subtracted. The agreement of these two values implies that the model used here represents the adsorbed amount of F127 well. It must be stressed that this value gives us the adsorbed amount per cm^3 of the dispersion and not an adsorbed amount per unit of SWCNT area, which is calculated to be 1.3 mg m^{-2} on the basis of the fit parameters in Table 1. This is thought to be a reasonable value for the adsorbed amount when compared to values for adsorbed amounts in the literature, as mentioned earlier, particularly a value obtained by Granite et al. of 1.80 mg m^{-2} and a value obtained by Lin and Alexandridis for adsorbed F127 onto carbon black of 0.543 mg m^{-2}.[7,17]

From the experimental data studied here, SANS data fitting is consistent with small SWCNT bundles in solution (of radius 10 Å), surrounded by a diffuse, water-swollen F127 adsorbed layer (of thickness 61 Å) and an adsorbed amount of 1.3 mg m^{-2}. These results are in general agreement with the main conclusions of Granite et al., and the adsorbed amount is consistent with previously reported values for F127 adsorption

DOI: 10.1021/acs.langmuir.5b00375
Langmuir 2015, 31, 3262−3268

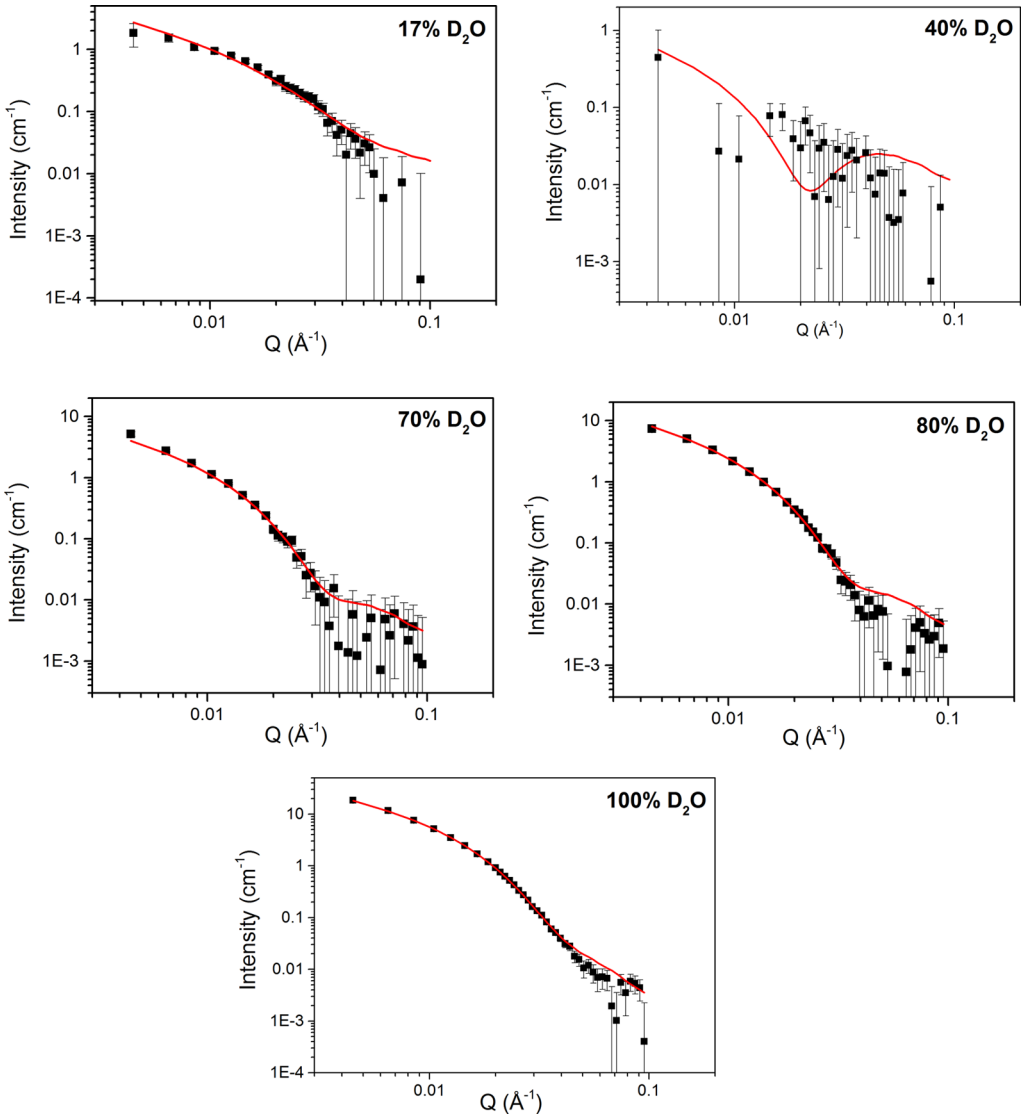

Figure 6. Scattering curves for F127-decorated SWCNTs at the five contrasts studied, with the core−shell cylinder fits described in Table 1.

on other substrates.[17] This finding is in contrast to previous work on the adsorption of small-molecule surfactants on SWCNTs, which are thought to form a dense, thin adsorbed layer on the surface of SWCNTs.[3]

CONCLUSIONS

SWCNTs dispersed with F127 pluronic block copolymer were investigated using small-angle neutron scattering. In this work, we have shown that our data agreed with the predicted scattering for a SWCNT core surrounded by a diffuse polymer layer, with minimal scattering being seen at a D_2O composition of 40%, as expected for core−shell cylinders of this type. The SANS data fitting is consistent with small SWCNT bundles in the dispersion, stabilized with an adsorbed F127 layer which is extended (with 61 Å thickness) and water-swollen (with a water content of 94% in the adsorbed layer).

Absorption spectra of the samples studied with SANS show no differences between the peaks of the samples made in D_2O compared to those made in H_2O. The peaks seen in these spectra are consistent with a high degree of debundling, although we believe they are too broad for single tubes, consistent with the parameters obtained when fitting the SANS data using the core−shell cylinder model.

The adsorbed layer fits the core−shell cylinder model well, with the adsorbed layer having a thickness and volume fraction of F127 which fit previous literature values. SWCNT/F127 samples were stable for many months after their initial dispersion, hence F127 is a suitable steric stabilizer for SWCNTs. These results show that the analysis of F127 adsorption onto SWCNTs can be simplified by using a core−shell cylinder model to characterize the adsorbed layer, which could have wider applications for the analysis of other adsorbed molecules onto carbon nanotubes.

ASSOCIATED CONTENT

Supporting Information

Transmission electron microscopy, small-angle X-ray scattering, small-angle neutron scattering, and SLD calculations for SWCNTs. This material is available free of charge via the Internet at http://pubs.acs.org.

DOI: 10.1021/acs.langmuir.5b00375
Langmuir 2015, 31, 3262−3268

AUTHOR INFORMATION

Corresponding Authors

*E-mail: E.Kastrisianaki-Guyton@bristol.ac.uk.
*E-mail: J.S.van-Duijneveldt@bristol.ac.uk.

Notes

The authors declare no competing financial interest.

ACKNOWLEDGMENTS

This work was funded by an EPSRC Industrial CASE Award (EP/G501467/1) and EPSRC DTA (EP/K502996/1), both sponsored by Merck Chemicals Ltd. We thank the Science and Technology Facilities Council for the allocation of beam time, travel, and consumables (experiment number RB1410067). This work benefited from SasView software, originally developed by the DANSE project under NSF award DMR-0520547. We thank Dr. Sean Davis and Mr. Jonathan Jones (Electron and Scanning Probe Microscopy Facility) for advice and for high-resolution TEM images. We also thank Prof. R. Richarson for access to small-angle X-ray scattering equipment and Mr. J. Hallett for running the SAXS samples. The Ganesha X-ray scattering apparatus used for this research was purchased under EPSRC Grant "Atoms to Applications" Grant ref. EP/K035746/1.

REFERENCES

(1) Iijima, S. Helical microtubes of graphitic carbon. *Nature* **1991**, *354*, 56−58.
(2) Saito, R.; Fujita, M.; Dresselhaus, G.; Dresselhaus, M. S. Electronic structure of chiral graphene tubules. *Appl. Phys. Lett.* **1992**, *60*, 2204−2206.
(3) Yurekli, K.; Mitchell, C. A.; Krishnamoorti, R. Small-angle neutron scattering from surfactant-assisted aqueous dispersions of carbon nanotubes. *J. Am. Chem. Soc.* **2004**, *126*, 9902−9903.
(4) Angelikopoulos, P.; Bock, H. Directed self-assembly of surfactants in carbon nanotube materials. *J. Phys. Chem. B* **2008**, *112*, 13793−13801.
(5) Yasin, S.; Luckham, P. Investigating the effectiveness of PEO/PPO based copolymers as dispersing agents for graphitic carbon black aqueous dispersions. *Colloids Surf., A* **2012**, *404*, 25−35.
(6) Islam, M. F.; Rojas, E.; Bergey, D. M.; Johnson, A. T.; Yodh, A. G. High Weight Fraction Surfactant Solubilization of Single-Wall Carbon Nanotubes in Water. *Nano Lett.* **2003**, *3*, 269−273.
(7) Granite, M.; Radulescu, A.; Pyckhout-Hintzen, W.; Cohen, Y. Interactions between block copolymers and single-walled carbon nanotubes in aqueous solutions: a small-angle neutron scattering study. *Langmuir* **2011**, *27*, 751−759.
(8) Mantid; http://www.mantidproject.org.
(9) Heenan, R. K.; Rogers, S. E.; Turner, D.; Terry, A. E.; Treadgold, J.; King, S. M. Small angle neutron scattering using Sans2d. *Neutron News* **2011**, *22*, 19−21.
(10) Alexandridis, P.; Holzwarth, J. F.; Hatton, T. A. Micellization of poly(ethylene oxide) -poly(propylene oxide) -poly(ethylene oxide) triblock copolymers in aqueous solutions: thermodynamics of copolymer association. *Macromolecules* **1994**, *27*, 2414−2425.
(11) Schaefer, D. W.; Brown, J. M.; Anderson, D. P.; Zhao, J.; Chokalingam, K.; Tomlin, D.; Ilavsky, J. Structure and dispersion of carbon nanotubes. *J. Appl. Crystallogr.* **2003**, *36*, 553−557.
(12) Wang, H.; Zhou, W.; Ho, D. L.; Winey, K. I.; Fischer, J. E.; Glinka, C. J.; Hobbie, E. K. Dispersing Single-Walled Carbon Nanotubes with Surfactants: A Small Angle Neutron Scattering Study. *Nano Lett.* **2004**, *4*, 1789−1793.
(13) Backes, C.; Bosch, S.; Udo, M.; Hauke, F.; Hirsch, A. Density gradient ultracentrifugation on carbon nanotubes according to structural integrity as a foundation for an absolute purity evaluation. *ChemPhysChem* **2011**, *12*, 2576−2580.
(14) Lingam, K.; Podila, R.; Loebick, C.; Chen, P.; Ke, P.-C.; Powell, B.; Pfefferle, L.; Rao, M. L. Effect of bundling on the π plasmon energy in sub-nanometer single wall carbon nanotubes. *Carbon* **2011**, *49*, 3803−3807.
(15) *SasView*; http://www.sasview.org/.
(16) Malmsten, M.; Linse, J. P.; Cosgrove, T. Adsorption of PEO-PPO-PEO block copolymers at silica. *Macromolecules* **1992**, *25*, 2474−2481.
(17) Lin, Y.; Alexandridis, P. Temperature-dependent adsorption of Pluronic F127 block copolymers onto carbon black particles dispersed in aqueous media. *J. Phys. Chem. B* **2002**, *106*, 10834−10844.
(18) Nelson, A.; Cosgrove, T. Small-angle neutron scattering study of adsorbed pluronic tri-block copolymers on laponite. *Langmuir* **2005**, *21*, 9176−9182.
(19) Liang, X.; Mao, G.; Ng, K. Y. S. Effect of chain lengths of PEO-PPO-PEO on small unilamellar liposome morphology and stability: an AFM investigation. *J. Colloid Interface Sci.* **2005**, *285*, 360−372.

DOI: 10.1021/acs.langmuir.5b00375
Langmuir 2015, 31, 3262−3268